

MACROCELL CORROSION OF STEEL IN CONCRETE – EXPERIMENTS AND NUMERICAL MODELLING

S. Jäggi ¹⁾, H. Böhni ¹⁾ and B. Elsener ^{1), 2)}

1) *Institute of Materials Chemistry and Corrosion, Swiss Federal Institute of Technology, ETH Hönggerberg, CH-8093 Zurich (Switzerland)*

2) *Department of Inorganic and Analytical Chemistry, University of Cagliari, I-09042 Monserrato (Cagliari, Italy)*

Abstract

Macrocell corrosion with a local anode and a large cathode frequently occurs in chloride induced corrosion of rebars in concrete and is responsible for very high local corrosion attacks and reduction in cross section of the rebars found e.g. in bridge decks or substructures. In model macrocells in mortar and in concrete the influence of resistivity, temperature and geometrical arrangement (area ratio between cathode and anode, location of cathode) on macrocell current and its distribution on the cathode has been studied. The cathodic oxygen reduction reaction and the anodic dissolution of the steel in pitting conditions have been studied separately and used as input data for the numerical modelling of the macrocell with the same geometrical anode / cathode arrangements as the mortar experiments. A very good agreement between modelling and experiments was found for the total macrocell current, its distribution and its temperature dependance. This numerical approach allows to perform parameter studies very rapidly and to design experiments with macrocells in concrete in a rational way.

Keywords

Macrocell, current distribution, concrete resistivity, modelling, oxygen reduction

Introduction

Reinforcing steel in good quality concrete does not corrode even if sufficient moisture and oxygen are available. This is due to the spontaneous formation of a thin protective oxide film (passive film) on the steel surface in the highly alkaline pore solution of the concrete. When sufficient chloride ions (from deicing salts or from sea water) have penetrated to the reinforcement or when the pH of the pore solution drops to low values due to carbonation, the protective film is destroyed and the reinforcing steel is depassivated. Corrosion in the form of rust formation and / or loss in cross section of the rebars occurs in the presence of oxygen and water (humidity) [1 - 3]. The corrosion of steel in concrete essentially is an electrochemical process, where at the anode iron is oxidized to iron ions that pass into solution and at the cathode oxygen is reduced to hydroxyl ions. Anode and cathode form a short circuited corrosion cell, with the flow of electrons in the steel and of ions in the pore solution of the concrete [1 – 3].

According to the different spatial location of anode and cathode, corrosion of steel in concrete can occur in different forms:

- as microcells, where anodic and cathodic reactions are immediately adjacent, leading to uniform iron dissolution over the whole surface. Uniform corrosion is generally caused by carbonation of the concrete or by very high chloride content at the rebars.

- as macrocells, where a net distinction between corroding areas of the rebar (anode) and non-corroding, passive surfaces (cathode) is found. Macrocells occur mainly in the case of chloride induced corrosion (pitting), generally the anode is small respect to the total (passive) rebar surface.



Figure 1: Localized corrosion attack on a 20 mm rebar, loss in cross section ca. 30%

On reinforced structures and in the experimental study of macrocells, coplanar or face to face situations of anode and cathode can be distinguished [4 – 6]. A typical coplanar situation is a localized corrosion attack in an otherwise passive rebar (figure 1), a typical face to face situation is the corroding upper layer of the reinforcement in a bridge deck with the lower mat being passive. Macrocell corrosion is of great concern because the local dissolution rate (reduction in cross section of the rebar) may greatly be accelerated due to the large cathode / anode area ratio [4 - 6]. Indeed, values of local corrosion rates up to 1 mm/year have been reported for bridge decks, sustaining walls or other chloride contaminated RC structures [7 - 9]. This rapid corrosion attack may lead – if not detected early – to structural safety problems.

Macrocell corrosion can be considered like a battery, the total current flowing, I_{ME} , is given by the driving voltage (potential difference between uncoupled anode and cathode) ΔU divided by the resistance of the electrolyte R_{EI} , the resistance of the anodic $R_A(i)$ and the cathodic reaction $R_C(i)$:

$$I_{ME} = \Delta U / (R_{EI} + R_A(i) + R_C(i)) \quad \text{eq. (1)}$$

In the literature, values between 0.25 and 0.5 V are reported for the driving voltage ΔU [10, 11]. The resistance of the electrolyte R_{EI} contains the geometry factor anode / cathode (e.g. increases for small anodes) and the mortar or concrete resistivity. The influence of porosity (w/c ratio, hydration...), relative humidity and temperature on the resistivity of cement based materials is well known [12, 13]. The temperature dependance of the electrolyte resistance can be written as

$$R_{EI} = R_{EI,0} * \exp(b [1/T - 1/T_0]) \quad \text{eq. (2)}$$

For reference temperature $T_0 = 20$ °C values of the constant b in the range of 1700 K (synthetic pore solution, pH 13.5) and 3800 K (concrete exposed for long time at 60% RH) have been reported [12, 13]. The cathodic oxygen reduction and especially its temperature dependance has not yet been studied extensively, only few data on tafel slope are available [14]. Corresponding data for the anode reaction in mortar or concrete are missing. For the temperature dependance of the two electrochemical reactions and of the total macrocell current an equation similar to eq. (2) can be written with the constant in the arrhenius equation called a:

$$I = I_0 / \exp(a [1/T - 1/T_0]) \quad \text{eq. (3)}$$

The aim of this work was to investigate the temperature dependence of the cathodic and the anodic reaction in the macrocell and to provide the necessary input data for the numerical modelling. The intensity and the temperature dependence of the macrocell current I_{ME} and the current distribution on the cathode are evaluated by numerical modelling.

Experimental

Cathodic and anodic reaction

The reaction kinetics were studied with potentiodynamic polarization curves in a conventional three electrode electrochemical cell in a thermostatic bath in order to vary the temperature. The reference electrode was a saturated calomel electrode. The cathodic reaction was studied on polished mild steel in synthetic pore solution with pH 13.5 [14] open to air or deaerated with Argon gas. The anodic reaction was studied in 0.1 M HCl.

Measurements of the cathodic polarization curves in mortar were performed with specially designed cylindrical mortar sample with a diameter of 4 cm. In the centre a degreased rebar sample (\varnothing 1 cm) was mounted, the counter electrode was a stainless steel grid (\varnothing 2.5 cm) and as reference electrode a small piece of activated titanium was used. The mortar samples (400 kg OPC/m³, w/c 0.6, cement / sand 0.25) were cured for 28 days at 80% relative humidity before starting the measurements.

All the potentiodynamic measurements started at the open circuit potential, the sweep rate was 1 mV/sec. The potentials reported are referred to saturated calomel electrode and corrected for the ohmic potential drop.

Macrocell investigations

The influence of temperature on macrocell corrosion has been studied for steel in mortar with the experimental setup reported previously [15].

A linear macrocell arrangement was prepared as mortar block of 30 x 30 mm with a length of 34 cm. It contained a segmented cathode (10 electrically isolated segments of 25 mm length) and in the centre an anode of 10 mm length (precorroded, embedded in a chloride containing mortar). The cover depth in this case was 1 cm.

A more realistic two- and three-dimensional macrocell arrangement was prepared in mortar blocks of 55 x 55 cm with a height of 15 cm, the cover depth was 7 cm on both sides.

The total macrocell current and the currents to the individual cathode segments were measured with a zero resistance ammeter, and the switching was performed on a programmable multimeter (Keithley). A special switchboard guaranteed a complete short circuit during the measurements. Data were recorded on a personal computer. The corrosion potentials of the anode and cathodes were measured with a saturated calomel electrode (SCE).

Numerical modelling

The numerical modelling was performed with a commercial boundary element program BEASY Corrosion and Cathodic Protection Design (Computational Mechanics, Ashurst, England). As input parameters the anodic and cathodic polarization curves determined in the experiments were used.

Experimental and modelling results

Cathodic oxygen reduction

The polarization curves of the oxygen reduction reaction and its temperature dependence have already been published [14, 15]. The curves showed as expected a Tafel behaviour for low overvoltages followed by a potential range with a diffusion limited current density. The Tafel slope increased with increasing prepassivation time to values higher than 240 mV/dec. Interesting to note that the diffusion limited current density was practically independent of temperature in the range of 5 – 50 °C.

The cathodic oxygen reduction in mortar showed lower current densities than in solution. The current densities increased with increasing temperature. The diffusion limited current density was found only at potentials < 0.8 V SCE or at very low oxygen content. The temperature dependence – obtained by normalizing to the cathodic current density at 20 °C – was identical in solution and in mortar (figure 3).

Anodic iron dissolution

The polarization curve of the anodic iron dissolution in 0.1 M HCl are shown in figure 4. The Tafel slope is about 75 mV/dec at 20°C and becomes lower with increasing temperature. The temperature dependence, normalized for a current density at 20°C, is shown in fig. 3.

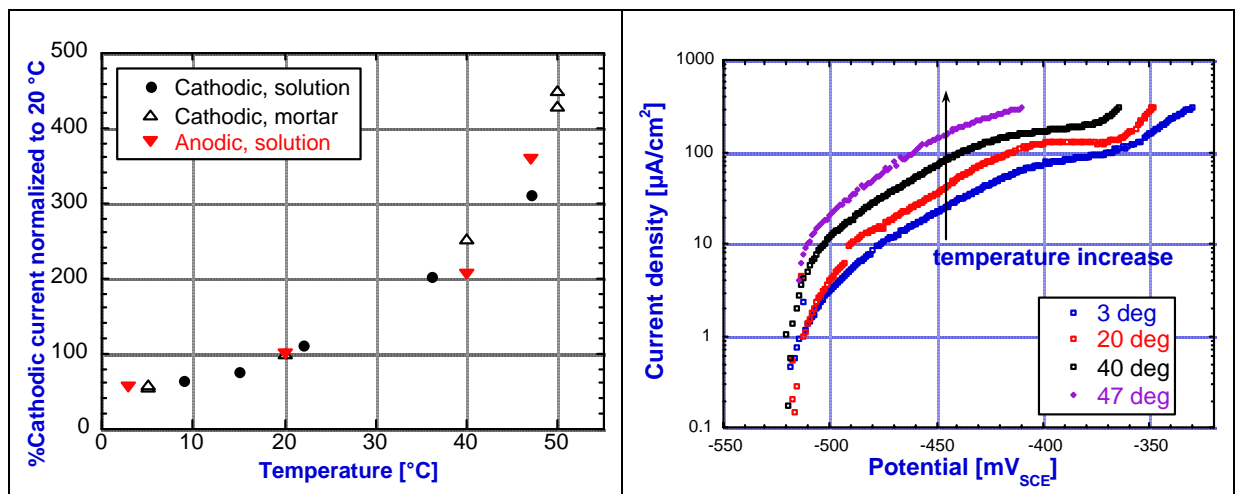


Figure 3: Normalized temperature dependence of the anodic iron dissolution and the cathodic oxygen reduction in solution and in mortar

Figure 4: Anodic polarization curves of rebar in 0.1 M HCl at different temperatures. Scan rate 1 mV/sec.

Macrocell corrosion current

The macrocell corrosion current measured between anode (rebar of 10 cm² area embedded in chloride contaminated mortar) and cathode (rebar of in synthetic pore solution, aerated) is shown in figure 5 together with the temperature variation over time. The macrocell current for the five (in principle identical) individual macrocells differs in intensity (probably due to a different size of the effective anode area) but the temperature dependence is similar; it is evident that the macrocell current increases with increasing temperature. The highest values measured were 120 µA at 50°C, demonstrating very high corrosion rates. Further the macrocell current remains fairly constant over the whole measuring periode (e.g. compare the currents at 10 °C at the beginning and at 250 hours).

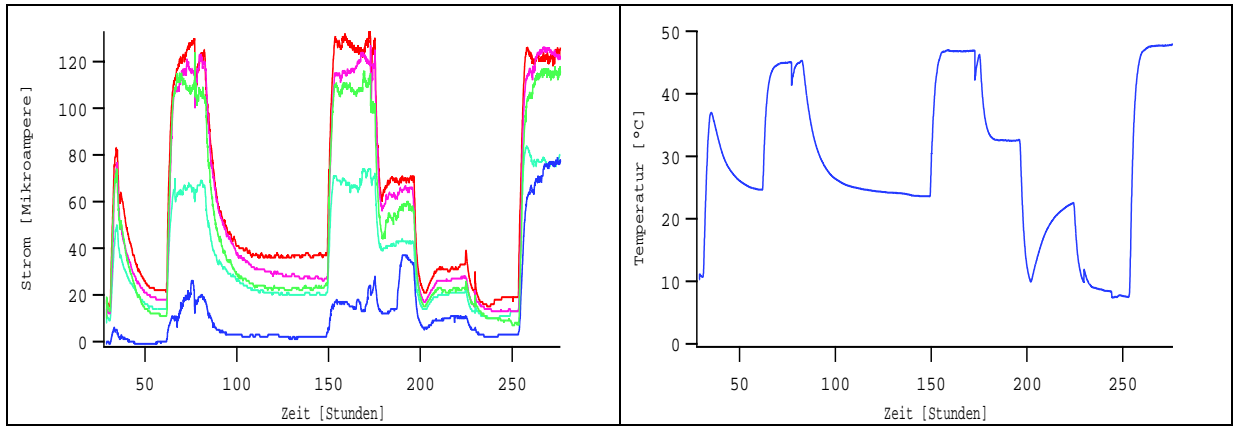


Figure 5: Macrocell current of five macrocells in synthetic pore solution (left) and temperature program versus time (right).

As for the anodic and cathodic reactions, the macrocell currents were normalized to the value at 20 °C, the resulting temperature dependence for the five macrocells is shown in **figure 6**. The constant of the arrhenius equation results in $a = 4350 \pm 80$ K in the same range as for the anodic and cathodic reactions (fig. 3).

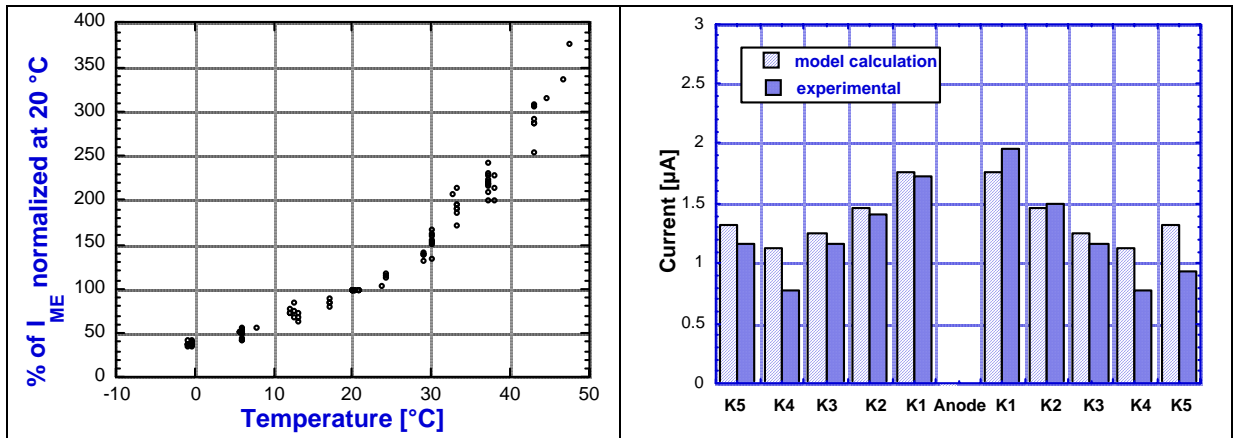


Figure 6: Normalized temperature dependance of the macrocell current measured in solution

Figure 7: Distribution of the cathodic currents as a function of the distance from the anode, results from experiments of the one-dimensional macrocell in mortar and from the numerical model

Macrocell corrosion in mortar – one dimensional model

The segmented one dimensional model macrocell bar allows to determine the current distribution on the cathode as a function of the distance from the anode. The cathode current slightly decrease with time. The main effect is the decrease of the cathode currents with increasing distance from the anode, the cathode segments at the end of the bars showing higher currents (**figure 7**); this is due to the fact that the mortar block is 2 cm longer then the macrocell bar.

Modelling the same geometrical arrangement of the linear segmented macrocell with the boundry element program BEASY, using the mortar resistivity, the cathodic polarization curve for the cathode segments and the anodic polarization curve for the anode as input data, the macrocell current and its distribution was calculated. A very good agreement between experimental and calculated values of the cathodic current is found (fig. 7).

Macrocell corrosion in mortar – two dimensional model

The macrocell current in the two dimensional model macrocell was measured as a function of temperature in several experiments. The macrocell current increases with temperature. It is interesting to note is that even at temperatures as low as -10 or -20 °C a small macrocell current of some μA was still flowing (fig. 8). The temperature dependance of the macrocell current in the mortar block is identical with that found in solution (fig. 6), the coefficient of the Arrhenius equation describing the temperature dependance is 4209 ± 88 K.

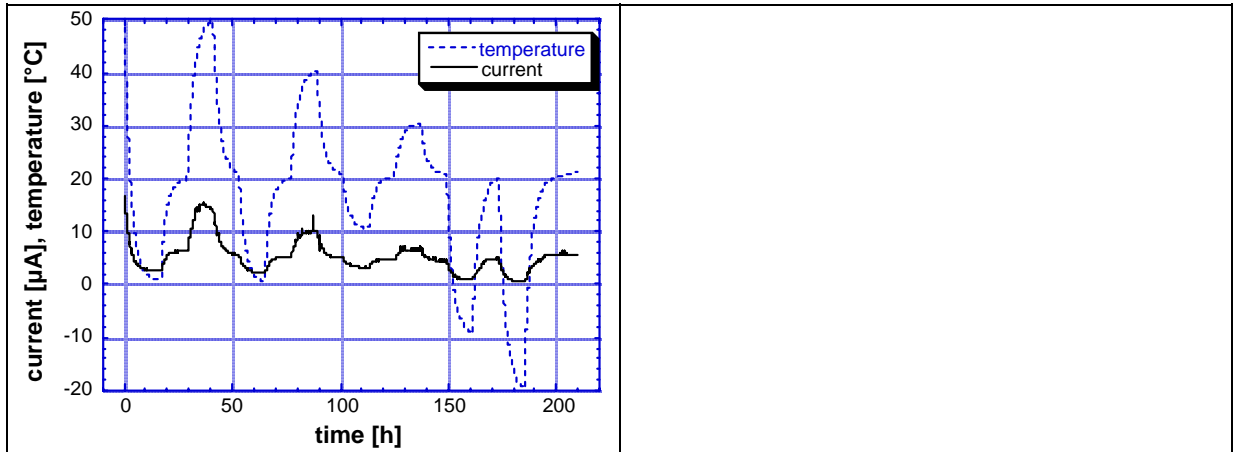


Figure 8: Macrocell current and temperature versus time, two dimensional macrocell in mortar. Area anode 3.1 cm^2 , area cathode 301 cm^2 , cover 7 cm.

The two dimensional macrocell was modelled numerically with the boundary element program BEASY, as input data the mortar resistivity, the polarization curve of the cathodic reaction for the cathode segments and the anodic polarization curve for the anode segment were used. The resulting current distribution is shown in figure 9. A gradual decrease from the centre (current density at the cathode $> 2.9 \mu\text{A}/\text{cm}^2$) to the end of the 55 cm long cathode bars (current density $< 2.3 \mu\text{A}/\text{cm}^2$) can be seen. The current distribution is symmetrical for all four directions; it further can be noted that the current density at the end of the bars is far from being negligible. The total macrocell current calculated with the numerical model as a function of temperature agrees well with the experimental results.

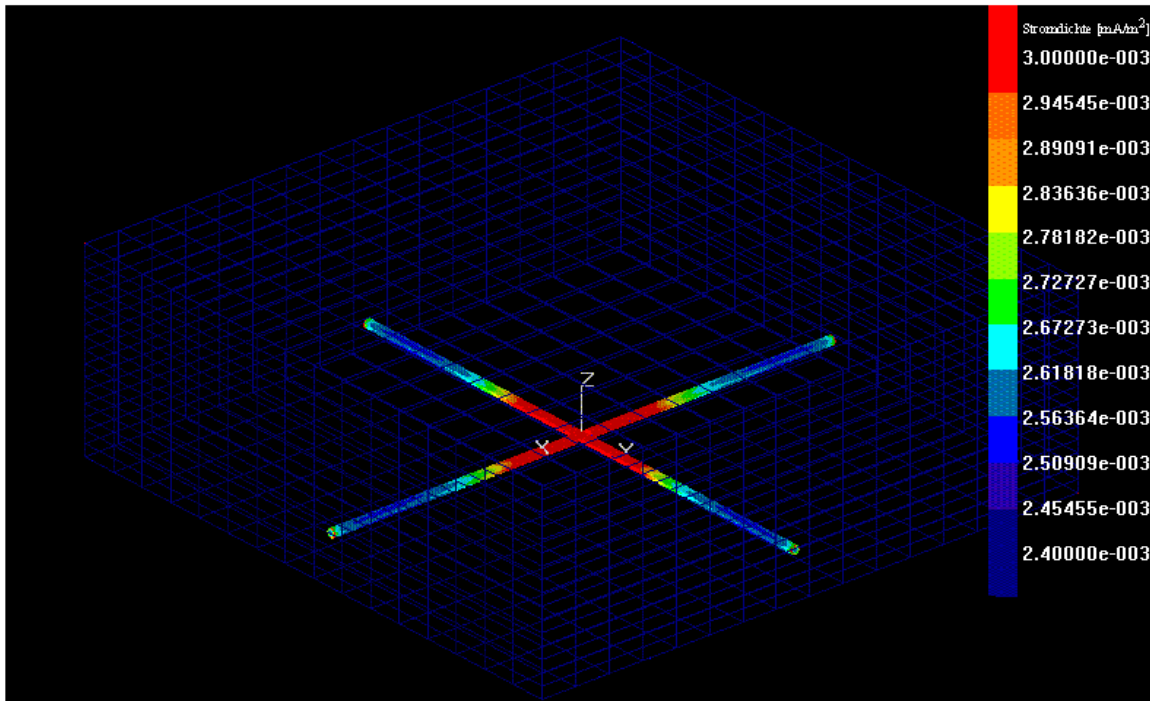


Figure 9: Numerical calculations with the boundary element program BEASY CP of the current distribution in a two-dimensional macrocell in a mortar block (cover 35 mm). Temperature 5 °C, total macrocell current 45.9 μ A, anode area 3.14 cm^2 .

Discussion

Macrocell corrosion between actively corroding areas of rebars and large passive areas (either beside the active spot or behind in a second layer of reinforcement) is of great concern because it results in very high local anodic current densities with corrosion rates up to 0.5 to 1 mm/year. The resulting local loss in cross section has dangerous implications for the structural safety if the corroded rebars are located in a zone of high tensile or shear stresses. Furthermore, these dangerous attacks very often do not manifest themselves at the concrete surface by cracking or spalling because soluble iron chloride complexes are formed [16]. The implications of these very inhomogeneous corrosion situation on the different monitoring techniques that allow to detect these locally corroding areas and quantify the local corrosion attacks – half cell potential mapping and polarization resistance measurements – have been presented recently [17].

In this work two new aspects arise: first, macrocell corrosion of steel in concrete has been studied for the first time in a wide range of temperatures, and second, the numerical modelling with the boundary element program is based not only on geometry (area ratio cathode / anode, cover depth) and concrete resistivity but also on the actual polarization curves of the cathodic and anodic areas. This allows to get much more significant results.

Temperature dependance

The temperature dependance of both the macrocell current and the anodic resp. cathodic partial reaction of the corrosion reaction of steel in concrete has been studied in a range of 0 to +50 °C. The coefficients a of the temperature dependance are summarized in [table 1](#). As can be noted, the temperature dependance of the anodic iron dissolution and the cathodic oxygen reaction in alkaline media as well as the total macrocell current in alkaline solution and mortar agree very well, a =

4280 ± 150 K. A comparison with literature results shows a good agreement (fig. 10), although it has to be noted that the temperature interval may influence on the calculated value of the temperature coefficient a . Numerical modelling of the macrocell with the polarization curve of the anodic and cathodic partial reaction and the mortar resistivity allowed to calculate the influence of temperature on the macrocell current, a very good agreement with the experimental results is observed (fig. 10). It is very interesting to note that the coefficients of temperature dependance calculated from macrocell currents measured between an anode in instrumented cores and the rebar network of bridge decks [22] is in good agreement with these laboratory results (tab. 1). The higher standard deviation results from different exposure conditions.

Table 1: Temperature dependance coefficient a (eq. 2) for anodic, cathodic and total macrocell current in solutions and mortar experiments

| Current / Media | solution | mortar 1-dim | mortar 2-dim | field 3-dim |
|-----------------|-----------|--------------|--------------|-----------------|
| Macrocell | 4350 ± 80 | | 4210 ± 90 | 4000 ± 250 [22] |
| Anodic | 4300 | - | - | - |
| Cathodic | 4310 | 4250 | - | - |

A comparison of the temperature dependance of the anodic and cathodic reactions and the macrocell current of steel in concrete with the temperature dependance of the mortar (at 85 % RH) is shown in figure 11. As can be noted, the temperature dependance is much more pronounced for the electrochemical reactions then for the mortar resistivity. This indicates that the proportionality between polarization resistance and concrete resistivity often reported in literature [23, 24] can not be assumed to be valid a priori or – in other words – for chloride induced corrosion the corrosion rates can not be calculated from concrete resistivity.

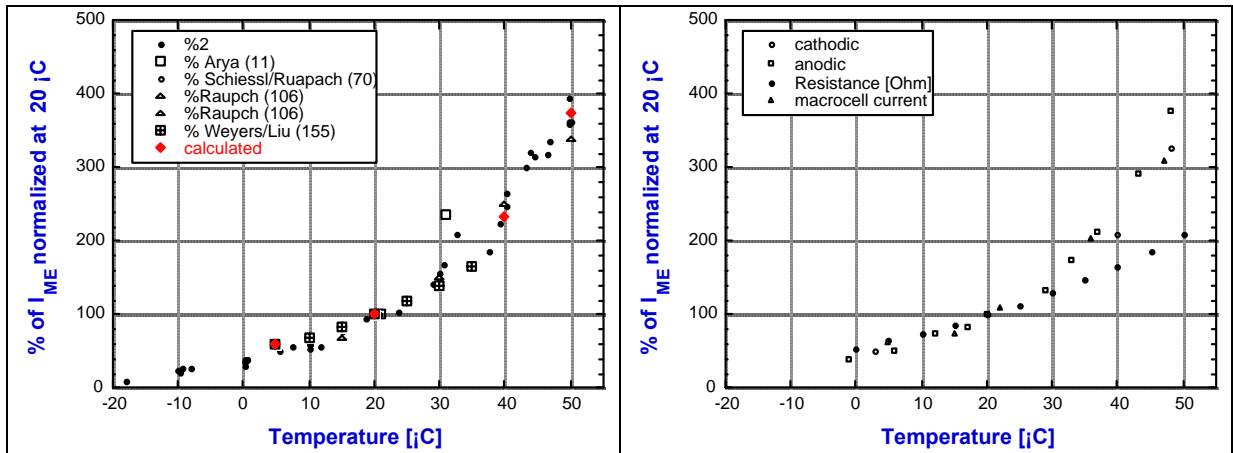


Figure 10: Temperature dependance of the macrocell current of steel in mortar and concrete. Comparison of literature values of Arya [18], Schiessl [19], Raupach [20], Weyers and Liu [21] with own experimental (●) and numerical (◆) results.

Figure 11: Temperature dependance of the anodic, cathodic and macrocell corrosion current compared to the temperature dependance of the concrete resistivity ($b = 3080$ K, RH 85%)

Rate controlling reaction step

According to eq. (1) the macrocell current is controlled by the electrolyte resistance R_{el} and the two polarization resistances of the anodic (R_a) and cathodic (R_c) reaction. Which one of these three resistances determines the overall macrocell current is still under discussion, often it is stated that the concrete resistance is the controlling factor for the corrosion rate of steel in concrete. From the results of this work it can be concluded that for large cathode areas and in mortar with a quite low resistivity of about $100 \Omega m$ (as if frequently occurs in chloride induced corrosion) it is the cathodic oxygen reduction reaction occurring on the passive reinforcement that is controlling the overall reaction (> 90% of the total resistance in eq. 1) whereas the part of the electrolyte resistance is only ca. 5 – 10%. The anode is practically not polarized. Numerical simulation with a plan-parallel arrangement of the electrodes [10] has also shown that the cathodic reaction controls the overall macrocell corrosion by more than 60%. The difference to this work arises from the different geometrical arrangement: the small anode in a relatively large mortar block (55 * 55 * 15 cm) has a lower resistive control than the plan-parallel arrangement.

It can further be concluded that the geometry used in laboratory studies with mortar beams or blocks can greatly influence the *experimental* results; similar the cathodic polarization curve (tafel slope, exchange current density) used as input data greatly influence the results of numerical modelling.

Advantages of numerical modelling

Numerical modelling of macrocell corrosion using a geometrical arrangement (size of the anode, cover depth, size and position of cathodes) and the polarization curve of the anode and the cathode together with concrete resistivity as input data has demonstrated to be a powerful tool in studying macrocell corrosion. The total macrocell current, its distribution on the cathode and its temperature dependance agreed very well with the laboratory experiments with identical parameters. This allows to change the usual way of doing experiments: based on a small set of input data first numerical modelling is performed for different geometries (e.g. long slabs, decks etc.) and for different concrete resistivities. In a second step the laboratory experiments are designed and the results of numerical modelling are verified.

Conclusions

In real structures with localized chloride induced corrosion macrocells are formed that greatly accelerate the local dissolution rate of the anode. From this work performed on active/passive model macrocells in the laboratory combined with numerical modelling it can be concluded:

1. The temperature dependance of anodic iron dissolution, of the cathodic oxygen reduction reaction and of the overall macrocell corrosion is nearly identical ($a = 4200 K$) and much higher than the temperature dependance of the mortar or concrete resistivity (RH 85%).
2. Numerical modelling with the boundary element program BEASY provides practically the same results for the total macrocell current, current distribution on the cathode and temperature dependance as found in the experiments in mortar for a given geometrical arrangement, concrete resistivity and cathodic polarization curves of the passive steel in concrete
3. Chloride induced macrocell corrosion in low to moderate resistive concrete is governed by the cathodic oxygen reduction reaction and not by concrete resistivity.
4. This numerical approach allows to perform parameter studies very rapidly and to design experiments with macrocells in concrete in a rational way.

References

- 1 K. Tuuti, Corrosion of Steel in Concrete, CBI Forskning/Research, April 1982, Cement och Betonginstitutet, Stockholm
- 2 P. Schiessl, Corrosion of Steel in Concrete, RILEM Technical Committee 60-CSC, Chapman and Hall, New York (1988)
- 3 B. Elsener, Corrosion of Steel in Concrete, in Corrosion and Environmental Degradation, ed. M. Schütze, Vol. II p. 389 – 436, WILEY-VCH Weinheim (2000)
- 4 C. Andrade, I.R. Maribona, S. Feliu, A. Gonzalez, S. Feliu Jr, Corrosion Science 33 (1992) 237
- 5 M. Raupach, Chloride induced macrocell corrosion of steel in concrete – theoretical background and practical consequences, Construction and Building Materials, 10 (1996) 329
- 6 B. Elsener, A. Hug, D. Bürchler and H. Böhni, Evaluation of Localized Corrosion Rate on Steel in Concrete by Galvanostatic Pulse Technique, Corrosion of Reinforcement in Concrete Construction, ed. C.L. Page, P.S. Bamforth and J.W. Figg, SCI, Cambridge (1996) pp. 264 – 272
- 7 B. Elsener and H. Böhni, Potential Mapping and Corrosion of Steel in Concrete, in "Corrosion Rates of Steel in Concrete", ASTM STP 1065, eds. N. S. Berke, V. Chaker and D. Whiting, American Society for Testing and Materials, Philadelphia, 1990, 143.
- 8 F. Hunkeler, Assessment of Corrosion on RC Structures with Potential Mapping (in German) Schweiz. Ingenieur und Architekt, 109 (1991) 272.
- 9 B. Elsener, Corrosion Rate on Reinforced Concrete Structures Determined by Electrochemical Methods, Materials Science Forum, 192 – 194 (1995) 857.
- 10 M. Raupach and J. Gulikers, Investigations on Cathodic Control of Chloride Induced Reinforcement corrosion, in Corrosion of Reinforcement in Concrete - Corrosion Mechanism and Protection, EFC Publication Nr. 31, ed. J. Mietz, R. Polder and B. Elsener, IOM Communication, London (2000) p. 13 - 23
- 11 B. Elsener, Corrosion rate of steel in concrete – from laboratory to reinforced concrete structures, in Corrosion of Reinforcement in Concrete, Monitoring, Prevention and Rehabilitation, ed. J. Mietz, B. Elsener and R. Polder, The Institute of Materials IOM Communications, London (1998) pp. 92 – 103
- 12 D. Bürchler, Der elektrische Widerstand von zementösen Werkstoffen, PhD Thesis No. 11876 (1996) ETH Zürich (in German)
- 13 D. Bürchler, B. Elsener and H. Böhni, Electrical Resistivity and Dielectric Properties of hardened cement paste and mortar, in Corrosion of Reinforcement in Concrete Construction, ed. C.L. Page, P. Bamforth and J.W. Figg, SCI, Cambridge (1996) p. 283 - 293
- 14 S. Jäggi, B. Elsener and H. Böhni, Oxygen reduction on mild steel and stainless steel in alkaline solutions, in Corrosion of Reinforcement in Concrete - Corrosion Mechanism and Protection, EFC Publication Nr. 31, ed. J. Mietz, R. Polder and B. Elsener, IOM Communication, London (2000) p. 3 - 12
- 15 S. Jäggi, Experimentelle und numerische Modellierung der lokalen Korrosion von Stahl in Beton unter besonderer Berücksichtigung der Temperaturabhängigkeit, PhD Thesis No. 14058 (2001) ETH Zürich (in German)
- 16 Guilbaud J.P., Chahbazian G., Derrien F., Raharinaivo A., Electrochemical Behaviour of Steel under cathodic protection in medium simulating concrete, Corrosion and Corrosion Protection of Steel in Concrete, ed. R.N.Swamy, Sheffield Academic Press, Vol.2, pp. 1382- 1391
- 17 B. Elsener, Macrocell corrosion of steel in concrete – implications for corrosion monitoring, Cement & Concrete Composites, (2001) p.
- 18 C. Arya, Cement and Concrete Research 25 (1995) 989
- 19 P. Schiessl, M. Raupach, Influence of Concrete Composition and Microclimate on Critical Chloride Content in Concrete, in Corrosion of Reinforcement in Concrete, C.L. Page, K.W. Treadaway, P.B. Bamforth eds. (1990) London, Elsevier Applied Science p. 49 – 58

- 20 M. Raupach, Results from Laboratory Tests and Evaluation of Literature on the Influence of Temperature on Reinforcement Corrosion, Corrosion of Reinforcement in Concrete, EFC Publication Nr. 25, J. Mietz, B. Elsener and R. Polder eds., IOM Communications London (1998) p. 9 – 20
- 21 T. Liu, R. W. Weyers, Cement and Concrete Research 28 (1998) 365 – 379
- 22 Y. Schiegg, B. Elsener and H. Böhni, Online-monitoring of the corrosion in reinforced concrete structures, Proc. EUROCORR 2001
- 23 C. Alonso, C. Andrade, J.A. Gonzalez, Cement and Concrete Research 18 (1988) 687 – 698
- 24 F. Hunkeler, Constr. Building Materials 10 (1996) 381 - 389